Original Article

A study to improve the image quality in low-dose computed tomography (SPECT) using filtration

SC Kheruka, UC Naithani[1], AK Maurya[2], NK Painuly[3], LM Aggarwal[4], S Gambhir

Departments of Nuclear Medicine and [2]Radiotherapy, SGPGIMS, Lucknow, [1]Department of Physics, HNB University, Srinagar, [3]Department of Radiotherapy, CSMMU, Lucknow, [4]Departments of Radiotherapy and Radiation Medicine, IMS, BHU, Varanasi, India

ABSTRACT

Background: The output of the X-ray tube used in computed tomography (CT) provides a spectrum of photon energies. Low-energy photons are preferentially absorbed in tissue; the beam spectrum shifts toward the higher energy end as it passes through more tissue, thereby changing its effective attenuation coefficient and producing a variety of artifacts (beam-hardening effects) in images. Filtering of the beam may be used to remove low-energy photon component. The accuracy of attenuation coefficient calculation by bilinear model depends highly upon accuracy of Hounsfield units. Therefore, we have made an attempt to minimize the beam-hardening effects using additional copper filter in the X-ray beam. The quantitative evaluation were made to see the effect of additional filters on resulting CT images. **Materials and Methods:** This study was performed on dual-head SPECT (HAWKEYE 4, GE Healthcare) with low-dose CT which acquires images at peak voltages of 120/140 kV and a tube current of 2.5 mA. For the evaluation of image quality, we used CT QA Phantom (PHILIPS) having six different density pins of Water, Polyethylene, Nylon (Aculon), Lexan, Acrylic (Perspex) and Teflon. The axial images were acquired using copper filters of various thicknesses ranging from 1 to 5 mm in steps of 1 mm. The copper filter was designed in such a manner that it fits exactly on the collimator cover of CT X-ray tube. Appropriate fixation of the copper filter was ensured before starting the image acquisition. As our intention was only to see the effect of beam hardening on the attenuation map, no SPECT study was performed. First set of images was acquired without putting any filter into the beam. Then, successively, filters of different thicknesses were placed into the beam and calibration of the CT scanner was performed before acquiring the images. The X-ray tube parameters were kept the same as that of unfiltered X-ray beam. All the acquired image sets were displayed using Xeleris 2 (GE Healthcare) on a high-resolution monitor. Moreover, Jaszak's SPECT Phantom after removing the spheres was used to see the different contrast intensities by inserting the different contrast materials of iodine and bismuth in water as background media. Images were analyzed for visibility, spatial resolution and contrast. **Results:** Successive improvement in the image quality was noticed when we increased the filter thickness from 1 to 3 mm. The images acquired with 3-mm filter appeared almost with no artifacts and were visibly sharper. Lower energy photons from X-ray beam cause a number of artifacts, especially at bone–tissue interfaces. Additional filtrations removed lower energy photons and improved the image quality. Degradation in the image quality was noticed when we increased the filter thickness further to 4 and 5 mm. This degradation in image quality happened due to reduced photon flux of the resulting X-ray beam, causing high statistical noise. The spatial resolution for image matrix of 512 × 512 was found to be 1.29, 1.07, 0.64 and 0.54 mm for without filter, with 1, 2 and 3 mm filters, respectively. The image quality was further analyzed for signal-to-noise ratio (SNR). It was found to be 1.72, 1.78, 1.98 and 1.99 for open, with 1, 2 and 3 mm filters respectively. This shows that 3-mm filter results in an improvement of 15.7% in SNR. **Conclusion:** On the basis of this study, we could conclude that use of 3-mm copper filter in the X-ray beam is optimal for removing the artifacts without causing any significant reduction in the photon flux of the resulting X-ray beam. We also propose that as artifacts have been removed from the images, the value of Hounsfield units will be more accurate and hence the value of attenuation coefficients lead to better contrast and visualization of SPECT images.

Keywords: Artifacts, attenuation correction, beam hardening, filtration, image quality, low-dose computed tomography

Access this article online

Quick Response Code:

Website: www.ijnm.in

DOI: 10.4103/0972-3919.84595

INTRODUCTION

The theoretical foundations for the tomographic image reconstruction were laid as early as 1917 when Radon described a transform which relates the properties of an object to projections measured at angles around the object.[1] This was later extended to X-ray imaging by Cormack.[2,3] At about the same time, Kuhl

Address for correspondence:
Dr. Subhash Chand Kheruka, Department of Nuclear Medicine, SGPGIMS, Lucknow – 226 014, India. E-mail: skheruka@yahoo.com

and Edwards used optical superposition to reconstruct slices from projections acquired with a rectilinear scanner.[4] While these pioneering works provided the foundation for computed tomography (CT). Later on Hounsfield described a method for obtaining tomographic slices with a rotating X-ray tube[5] that computer assisted tomography (CAT or CT) was established in medical imaging. The techniques developed for X-ray CT were subsequently applied to nuclear medicine by initially rotating the patient in front of the gamma camera detector and subsequently rotating the detector around the patient.[6-9] A detailed treatise on performing emission-CT with modified conventional gamma cameras, including instrumentation, acquisition and reconstruction implications was published by Larsson.[10] The technique of performing tomographic imaging of an isotope which emits single-energy photons with a rotating gamma camera is referred to as single photon emission computed tomography (SPECT). Most current commercial gamma cameras are available with SPECT capability. Traditionally, SPECT systems were based on a single rotating detector. The sensitivity of the gamma camera can be improved by using more than one detector. This also has the potential to reduce the study time and improve the quality of the study.

Photon attenuation and scattering are two of the most critical factors in achieving high quantitative accuracy in SPECT imaging. Photons emitted by radiopharmaceuticals can undergo photoelectric interaction with the inner-shell atomic electrons of a medium and get completely absorbed by the medium. On the other hand, photons can be Compton scattered when they interact with the loosely bound electrons in the medium. The energy of the scattered photons can be lower than or the same as that of the incident photons. In the body, due to the low atomic number (Z) composition of the soft tissue and water, Compton scattering dominates. Since these factors are related to the density and composition of the body tissues, it is crucial to have access to individual attenuation maps to account for the attenuation and scatter effects when high quantitative accuracy is desired. It requires accurate measurement of attenuation, particularly in highly heterogeneous areas (e.g. thorax). For non-uniform attenuation correction, usually a transmission study can be performed prior to the emission scan, but it doubles the time and increases the chance of misregistration. To overcome this problem, efforts have been made to perform simultaneous measurements of emission and transmission. Several radioisotopes have been employed for this purpose including ^{153}Gd (100 keV), ^{99m}Tc (140 keV), ^{241}Am (59 keV), and ^{57}Co (122 keV). The main drawback of this technique is that transmission data also are contaminated by scatter events from the higher energy windows. The situation is further complicated when the emission source or transmission source has multiple energy peaks due to downscatter from the upper energy and spillover from the lower energy windows. These contaminations in the transmission window hamper the reconstruction of the attenuation map.[11-14] The problem with this technique is requirement of frequent replacement of the transmission source which is not cost-effective for routine practice.

Recent advances in radionuclide imaging technology have provided a new and powerful tool to handle this dilemma: integrated SPECT/CT systems. This work was pioneered by Lang and Hasagawa *et al*.,[15] who, not only combined hardware components into an integrated system but also developed important algorithms for SPECT attenuation correction using CT images. This technology makes it possible to acquire physiologic and anatomic images in a registered format and fuse them so that precise anatomic localizations of radiopharmaceutical distributions can readily be visualized. An additional benefit of this technologic advance is that the anatomic images can be used to perform high-quality attenuation corrections of the radiopharmaceutical distributions. CT images are acquired as transmission maps with a high photon flux and are actually high-quality representations of tissue attenuation and thus can provide the basis for attenuation correction. Therefore, combining SPECT and CT modalities into an integrated system is a significant advancement because the two modalities are complementary in that the weaknesses of one are often the strengths of the other in specific imaging situations. CT images are acquired by using a high-output X-ray tube and an arc of detectors in a fixed geometry to acquire cross-sectional transmission images of the patient as the X-ray tube and detector configuration rapidly rotates around the patient as shown in Figure 1a and b. The integration of SPECT and CT systems into a single imaging unit sharing a common imaging table provides a significant advancement in technology because this combination permits the acquisition of SPECT and CT data sequentially in a single patient study, with the patient in an ideally fixed position. Thus, the two datasets can be acquired in a registered format by appropriate calibrations, permitting the acquisition of corresponding slices from the two modalities. The

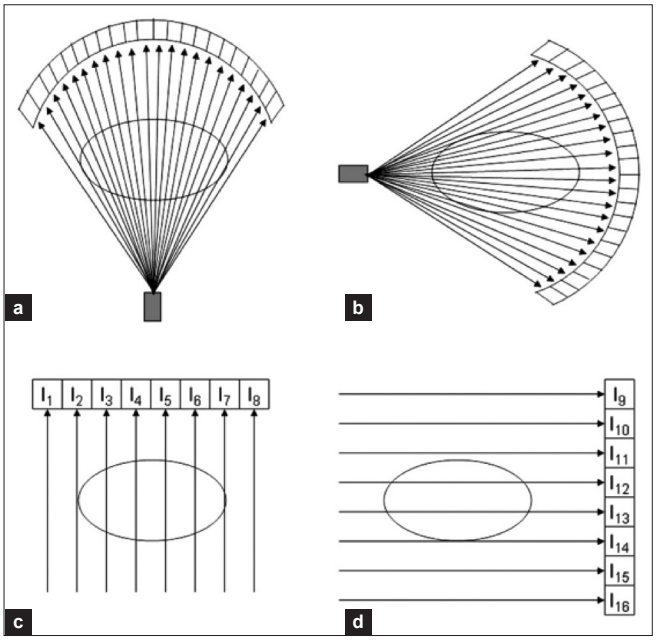

Figure 1: (a and b) CT data are acquired in fan beam geometry where individual rays represent transmitted photon intensities from multiple projections around patient. (c and d) These data can be reformatted into orthogonal geometry similar to that used for SPECT

CT data can then be used to correct for tissue attenuation in the SPECT scans on a slice-by-slice basis. Because the CT data are acquired in a higher-resolution matrix than the SPECT data, it is necessary to decrease the resolution of the CT data to match that of SPECT. In other words, the CT data are blurred to match the SPECT data. From the attenuation coefficient data acquired with CT, correction factors can then be determined as shown in Figure 2b, which can then be used to correct the SPECT data [Figure 2a] for attenuation, yielding the attenuation-corrected SPECT data as shown in Figure 2c. One additional topic must be addressed to ensure the accuracy of the attenuation correction. The output of the X-ray tube used in CT provides a spectrum of photon energies from 0 keV up to the maximum photon energy (kVp = peak energy in keV) setting used for the acquisition, as shown in Figure 3. Because low-energy photons are preferentially absorbed in tissue, the beam spectrum shifts toward the higher energy end as it passes through more tissue, thereby changing its effective μ and producing a variety of artifacts (beam-hardening effects) in images, and filtering of the beam to remove low-energy photons is required.

In the present work, we attempted to remove low-energy photons by introducing additional copper filters in the X-ray beam.

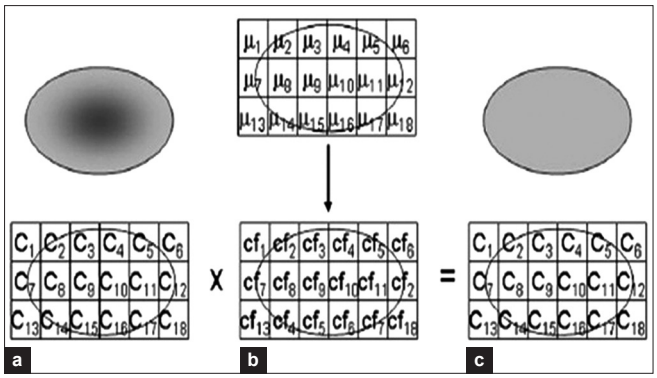

Figure 2: (a) Can be determined from attenuation coefficient measurements determined from CT scan and are used to correct emission counts from uncorrected SPECT scan; (b) Array of attenuation correction factors; (c) to provide final attenuation-corrected SPECT scan

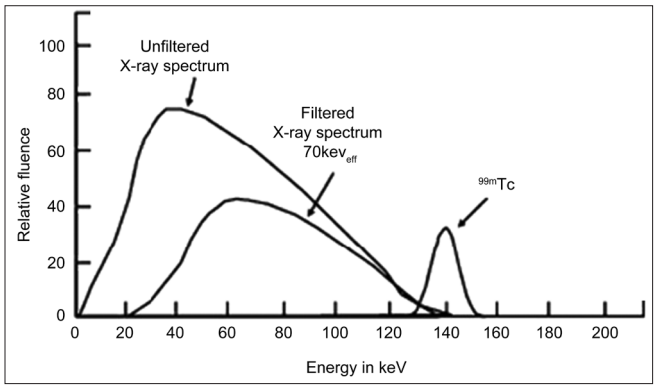

Figure 3: Typical energy spectrum of X-rays from X-ray tube. Filtered curve shows effects of filtration (beam hardening), which is used for CT. These data can be applied for attenuation correction of single-photon emitters such as ^{99m}Tc using bilinear model shown in Figure 6

MATERIALS AND METHODS

CT specification

This study was performed on dual-head SPECT system (HAWKEYE 4, GE Healthcare Technologies Waukesha, Wisconsin, USA) with low-dose MDCT (4-slice) [Figure 4]. The technical details of the CT scanner have been summarized in Table 1.

The use of a single gantry for the SPECT and CT systems results in a relatively low CT rotation speed of 23 s/rotation for the Hawkeye, as operated with heads opposite (H mode). Together with its X-ray tube operating only at 1.0–2.5 mA, exposures per rotation from 14.0 mA in half-rotation mode to 57.5 mA in full-rotation mode are achieved. Hence, the maximum exposure is roughly three times lower than in a typical diagnostic scan used in clinical routine (150 mA). The Hawkeye image slice width is fixed at 5.0 mm, whereas the slice width in diagnostic scanners is usually variable over a wide range. For tomographic image reconstruction, there are three frequency filters available for the Hawkeye, called "std" (standard), "soft" and "bone". The matrix dimension of the reconstructed image is 512 × 512 pixels.

Attenuation correction using CT

CT-based attenuation correction in SPECT–CT is much faster and introduces far less noise than the attenuation correction

Figure 4: SPECT–CT system

Table 1: Technical details of low-dose MDCT scanner

	Scan modes	Reconstruction filters	Detecto pitch at isocentre (mm)	Slice width (mm)	Tube voltage (KV)	Tube current (mA)	Time/Rotation (seconds)	mAs
Hawkeye 4	Axial half axial full helical (pitch = 1.923 cm)	Standard soft, Bone	1.19	5.0	120,140	1.0-25	14.0 23 23	14-35.0 23-57.5 2-30

MDCT = Multi-Detector CT

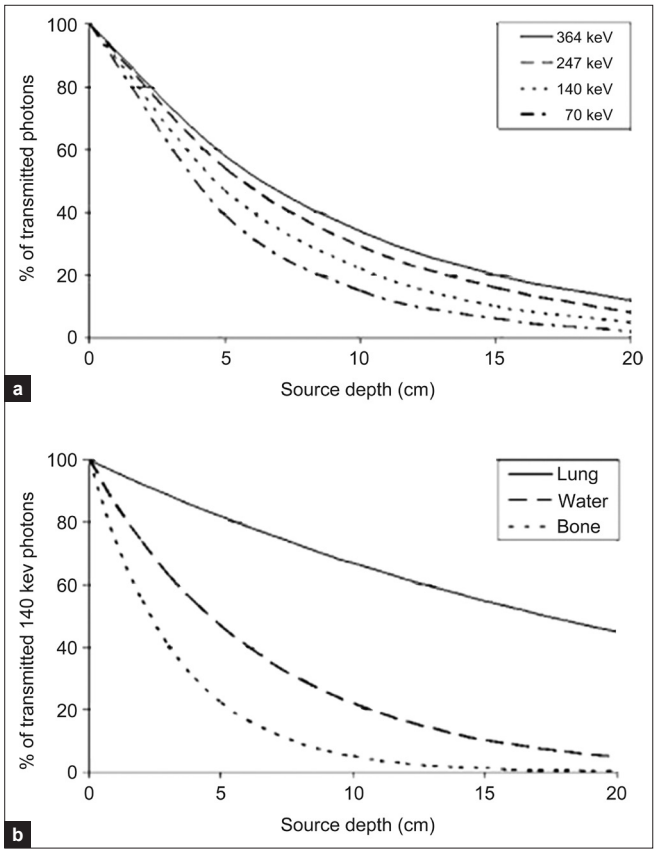

Figure 5: (a) Plot of percentage of transmitted photons as function of depth in 20-cm cylindrical Phantom measured in single planar projection image for radionuclides commonly used in nuclear medicine. (b) Plot of percentage of transmitted photons from ^{99m}Tc source as function of depth in lung, water, and bone

based on transmission scans in standalone SPECT systems. However, the sensitivity of the CT to dense materials such as metal implants and the conversion from CT Hounsfield units to SPECT attenuation correction factors can produce artifacts. The traditional approach is to start from the (diagnostic) CT image and derive an attenuation map with reduced resolution.

Attenuation effects vary with energy, as shown in Figure 5 (a). In addition, the magnitude of the attenuation effect depends on the tissue type, as shown in Figure 5 (b). It is necessary to convert the attenuation data acquired with CT to match the energy of the radionuclide used in the SPECT acquisitions. This is typically accomplished by using a bilinear model[12-14] relating attenuation coefficients at the desired energy to CT numbers measured at the effective energy of the CT beam of X-rays, as shown in Figure 6. For CT numbers less than 0, the measured tissue is assumed to be a combination of air and water, and the attenuation coefficient at the desired energy (i.e. 140 keV) can be calculated from the CT number by the following equation:

$$\mu_{tissue,\,140keV} = \frac{CT\#*(\mu_{water,\,140keV} - \mu_{air,\,140keV})}{1000} \qquad \text{(Equation – 1)}$$

This equation describes the first component of the bilinear curve in Figure 6. For CT numbers greater than 0, the conversion is more complicated because the measured tissue is a combination

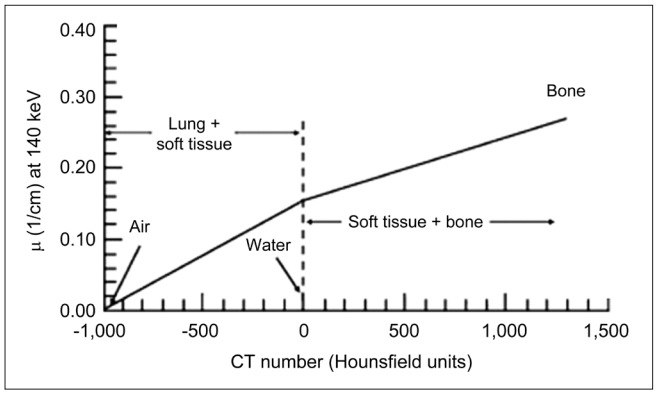

Figure 6: Bilinear model commonly used for converting measured CT numbers to attenuation coefficients for specific radionuclide such as ^{99m}Tc

of water and bone. In this case, the attenuation coefficient at the desired energy (140 keV) can be calculated from the CT number by the following equation:

$$\mu_{tissue,\,140keV} = \mu_{water,\,140keV} + \frac{CT\#*\mu_{water,keVeff}*(\mu_{bone,\,140keV} - \mu_{water,\,140keV})}{1000*(\mu_{tissue,\,keVeff} - \mu_{water,\,140keVeff})} \qquad \text{(Equation – 2)}$$

This equation describes the second component of the bilinear curve in Figure 6. In practice, the various attenuation coefficients for specific photon energy used in the SPECT acquisition and the effective photon energy used in the CT acquisition can be found in a stored look-up table in the reconstruction algorithm. The conversion can then be performed using two simple linear relationships relating the attenuation coefficient at the desired energy and the measured CT numbers for specific measured tissues. There are numerous advantages in the use of CT data for attenuation correction of emission data. First, the CT scan provides a high photon flux that significantly reduces the statistical noise associated with the correction in comparison to other techniques (e.g. radionuclides used as transmission sources). Also, because of the fast acquisition speed of CT scanners, the total imaging time is significantly reduced by using this technology. Another advantage related to the high photon flux of CT scanners is that attenuation measurements can be made in the presence of radionuclide distributions with negligible contributions from photons emitted by the radionuclides (i.e. post-injection CT measurements can be performed). The use of CT also eliminates the need for additional hardware and transmission sources that often must be replaced on a routine basis. Also, of course, the anatomic images acquired with CT can be fused with the emission images to provide functional anatomic maps for accurate localization of radiopharmaceutical uptake.

Contrast-to-noise ratio

The contrast-to-noise ratio (CNR) is an objective measure of the ability of an imaging system to detect large details. CNRs were determined by analyzing sectional images of the cylindrical syringe placed in water-filled Jaszak's Phantom and CT QA Phantom [Figure 7]. Circular regions of interest (ROIs) with

10 mm diameter were placed on the image of detail and on the background (BG) as indicated in Figure 8. Following the approach described by Gupta *et al.,*[15] CNRs were derived from mean CT numbers (CT) in the ROIs and the standard deviations (SD) in the background ROI as:

$$CNR = \frac{CT\#\,(Object) - CT\#\,(BG)}{SD\,(BG)}$$

Phantom studies

Study 1

As our intention was only to see the effect of beam hardening on the attenuation map, no SPECT study was performed. Phantom study 1 was performed to evaluate the performance of streak artifact suppression in the presence of very dense objects. To remove the low-energy photons from the X-ray beam, copper filters having thicknesses ranging from 1 to 5 mm were fabricated. The copper filters were designed in such a manner that they fit exactly on the collimator cover of CT X-ray tube. Appropriate fixation of the copper filter was ensured before starting the image acquisition. Water, iodine and bismuth contrast filled into three syringes of 2.5 ml having needles with lumen diameter of 24 gauge were introduced into a Jaszak's SPECT Phantom after removing the spheres. The cross-sectional area of the contrast-filled syringe was 54.11 mm^2. The water was filled in the Phantom to simulate the body. The concentrations of the iodine and bismuth contrast materials were 375 and 500 mg/ml, respectively. First, the Phantom was scanned without any additional copper filter into the X-ray beam. Then filters of copper ranging from 1 to 5 mm were introduced consecutively into the X-ray beam. The CT scanner was re-calibrated each time with the respective copper filter before scanning the Phantom. Images were analyzed for visibility, spatial resolution and contrast. To see the effect of heterogeneity interfaces on the image, cylindrical portion of the syringe having diameter of 8.3 mm with iodine concentration of 375 mg/ml inserted into the Phantom was used. The cross-sectional area of the contrast syringe has been assessed to see the effect of artifacts due to high–low density interfaces. All the acquired image sets were displayed using Xeleris 2 (GE Healthcare) on a high-resolution monitor.

Study 2

To verify the findings of the Phantom 1 study, we used CT QA Phantom (PHILIPS) having six different density rods of Water, Polyethylene, Nylon (Aculon), Lexan, Acrylic (Perspex) and Teflon. The Phantom was scanned first without any additional filtration of the X-ray beam. Then copper filter of 3-mm thickness was introduced and CT re-calibrated. The X-ray tube parameters were kept the same as those without copper filter. All the acquired image sets were displayed using Xeleris 2 (GE Healthcare) on a high-resolution monitor.

Figure 7: Jaszak's SPECT QA Phantom

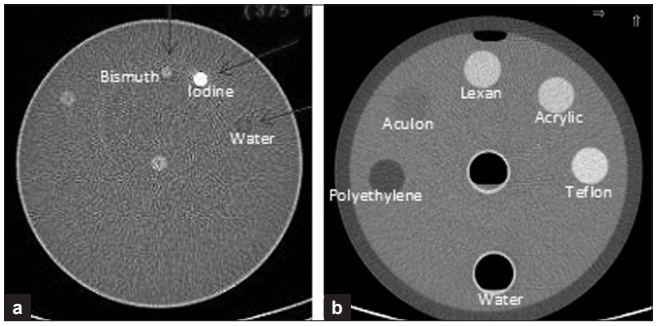

Figure 8: Cross-sectional views of the Phantoms: (a) Jaszak's Phantom; (b) CT Phantom

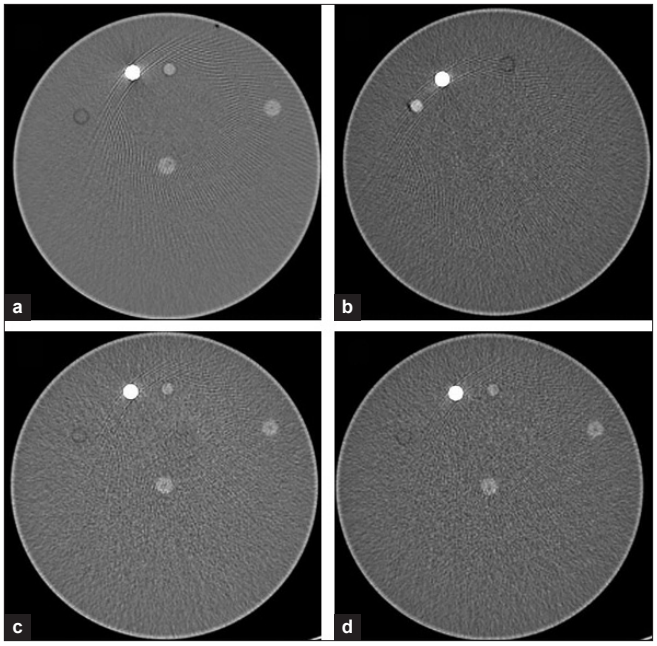

Figure 9: Acquired CT images of Jaszak's Phantom without and with different thickness of copper filters: (a) without filter (b) 1 mm (c) 2 mm (d) 3 mm

RESULTS

Phantom study 1

Successive improvement in the image quality was noticed when we increased the filter thickness from 1 to 3 mm. Basically, improvement in the image quality was noticed as reduction in streak artifacts which used to be very significant problem due to very fast attenuation of lower energy X-ray photons. The images

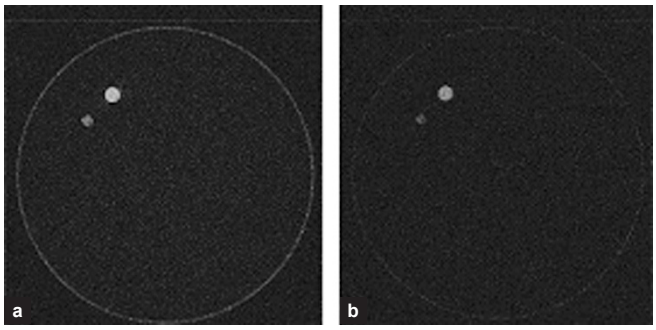

Figure 10: Cross-sectional images acquired with (a) 4 mm (b) 5 mm additional copper filter

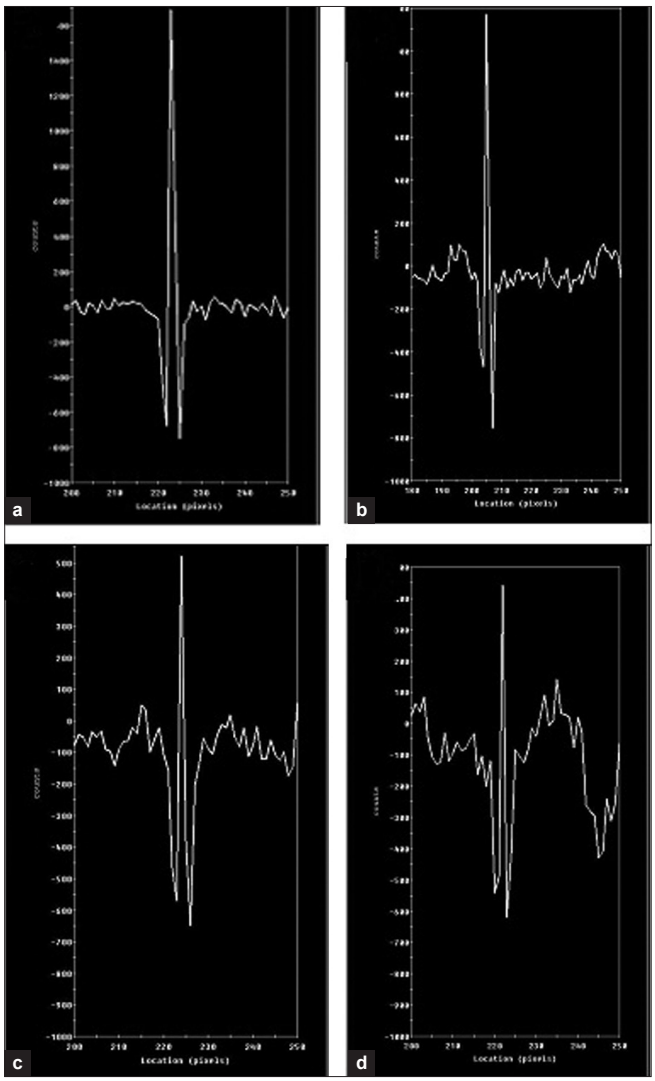

Figure 11: Spatial resolution spectrum: (a) open beam (b) 1 mm filter (c) 2 mm filter (d) 3 mm filter

acquired with 3-mm filter appeared almost with no artifacts and were visibly sharper [Figure 9a–d]. It was in accordance with our expectation as additional filtration removed lower energy photons from the resulting X-ray beam, causing a number of artifacts, especially at bone–tissue interfaces. A degradation in the image quality was noticed when we increased the filter thickness further [Figure 10]. We feel that this degradation in image quality

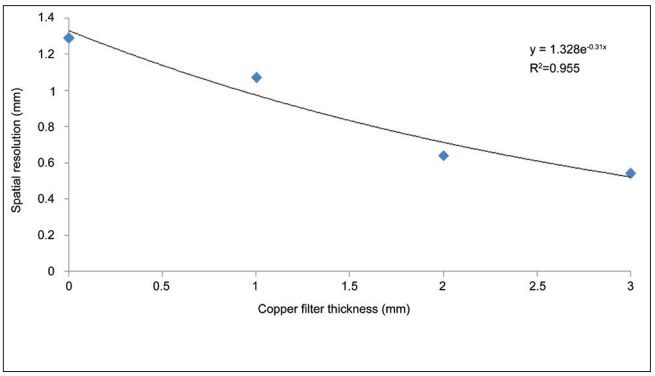

Figure 12: Spatial resolution versus additional copper filter thickness

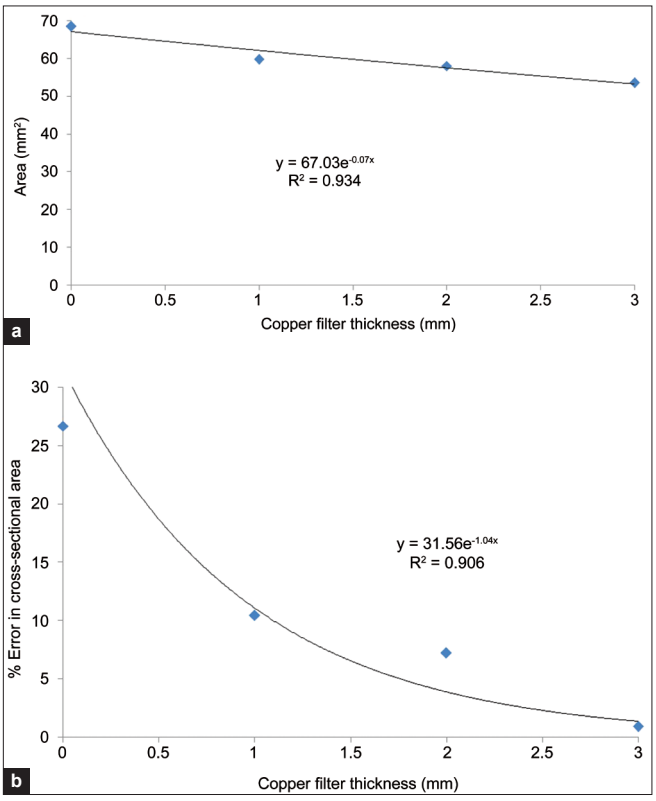

Figure 13: (a) Estimated cross-sectional area of the cylindrical syringe versus additional copper filter thickness. (b) % error reduction in area estimation versus additional copper filter thickness

happened due to reduced photon flux of the resulting X-ray beam, causing high statistical noise. The spatial resolution for image matrix of 512 × 512 was found to be 1.29, 1.07, 0.64 and 0.54 mm for without filter, with 1, 2 and 3 mm filter, respectively [Figure 11a–d]. The scatter graph of spatial resolution versus additional copper filter is shown in Figure 12. The cross-sectional areas measured on CT image of the iodine-contrast syringe have been found to be 68.55, 59.77, 58.01 and 53.61 mm^2 for without filter, with 1, 2 and 3 mm filters, respectively. The effects of additional copper filtration on area estimation have been plotted in Figure 13a and b. Due to lot of artifacts, the cross-sectional area of the contrast syringe measured on image without filter results in an error of 26.68%, whereas for the images with 1, 2 and 3 mm filters, the estimated error was found to be 10.46, 7.21

and 0.92%, respectively. This shows an improvement of 25.76% with 3-mm filter as compared to without any additional filter. The image quality was further analyzed for CNR for iodine-filled cylindrical syringe. It was found to be 18.31, 19.54, 20.06 and 23.49 for no additional filter, with 1, 2 and 3 mm filters, respectively. The effect of additional copper filtration on CNR has been plotted in Figure 14. This shows that 3-mm filter results in an improvement of 5.18 in CNR as compared to that without any additional filter.

Phantom study 2

The axial images acquired without any additional filter had a lot of streak artifacts, especially at metallic interfaces, due to beam-hardening effect. As expected from Phantom study 1, the axial image acquired with 3-mm filter was almost free from streak artifacts [Figure 15a and b]. The images were further analyzed for the CNR for the three rods of Lexan, Acrylic and Tefnol. Significant improvement in the CNR was found for all the three rods. The CNR value changed from 3.72 to 5.30, from 3.82 to 5.29 and from 4.15 to 7.51 for Lexan, Acrylic and Tefnol respectively [Table 2]. The resolution pattern was very clearly visualized in the cross-sectional image acquired with 3-mm copper filter compared to the image acquired without additional filter [Figure 16a and b].

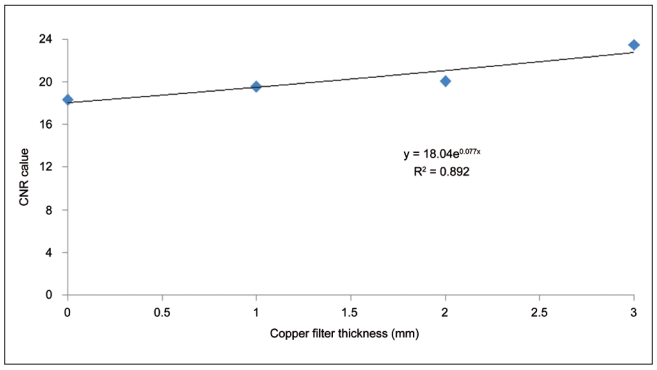

Figure 14: Contrast-to-noise ration versus additional copper filter thickness

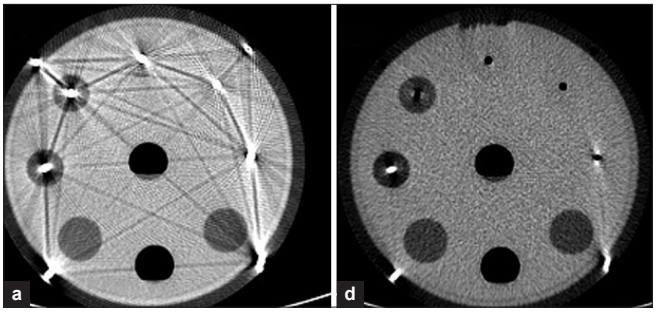

Figure 15: Streak artifacts on metal interfaces: (a) with no additional filter, (b) with additional 3-mm copper filter

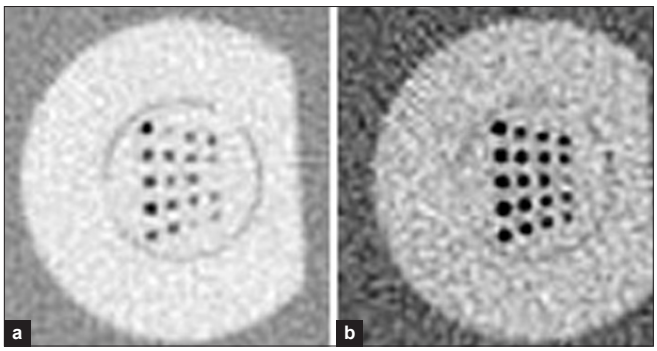

Figure 16: Visualization of resolution pattern: (a) without additional filter and (b) with additional 3-mm copper filter

Table 2: Contrast-to-noise ratio estimated from PHILIPS CT Phantom

Cylindrical rod material	CNR without additional filter	CNR with 3 mm copper filter
Nylon	3.72	5.30
Lexan	3.82	5.29
Acrylic	4.15	7.51

DISCUSSION

Beam hardening and scatter-induced artifacts in the CT image can have a similar appearance in the emission image. Metal artifacts in the CT image can severely distort the attenuation-corrected images, making these images effectively useless as reported by Johan Nuyts *et al.* on PET/CT images.[16]

These effects are illustrated with an abdominal test Phantom. Nowadays, full diagnostic CT units are combined with SPECT (e.g. Philips Precedence) and also in PET (e.g. GE Discovery). With the Hawkeye, however, GE offers a low-cost SPECT–CT unit where the CT scanner is mounted to the same gantry as the SPECT system and operates at low dose. The construction of the CT scanner differs significantly from conventional diagnostic CT units. The rotation speed of the Hawkeye gantry is 23 s/rotation, which is dramatically lower than the typical speed of modern diagnostic systems (<1 s/rotation). Apart from significantly prolonging the overall SPECT–CT scanning time (a scan of 40 cm corresponding to the SPECT axial field of view takes about 5 mins), CT image quality may be compromised by motion artifacts due to cardiac motion, breathing and voluntary movements.[17]

The maximum applicable dose of the Hawkeye X-ray tube is roughly three times smaller than the dose used in routine clinical diagnostic scans, although scans can be acquired at similar dose levels on diagnostic systems. It has to be noted, however, that a standard diagnostic system (with roughly three times higher dose) outperforms the Hawkeye significantly. In cases where patient dose is an issue, Hawkeye offers diagnostic advantages in low-contrast detail detection. Reduced radiation risk, however, has to be put into context of the overall patient exposure in a SPECT–CT examination. After all, it is a clinical decision if a patient would benefit from the information of a full diagnostic CT examination.

Attenuation correction problem in SPECT and PET imaging has been studied by several authors and various methods have been proposed to tackle this problem.[18-22] All manufacturers

of SPECT scanners incorporate X-ray CT-based attenuation correction algorithms in their systems, and for some PET scanners, it is the only option offered. The bilinear and hybrid scaling methods work well for clinical procedures where only biological materials are being imaged. There are remaining challenges, however, that can cause errors in the converted attenuation correction factors caused by contrast agents and respiratory motion as well as truncation and beam hardening. Errors that are present in the CT-based attenuation image have the potential of introducing bias or artifacts in the attenuation-corrected SPECT emission image as studied by Paul Kinahan *et al.* for PET/CT systems.[23] These effects are illustrated with an abdominal test Phantom containing aqueous F-18 FDG with a concentration of 4 kBq/ml, which is typical of a whole-body FDG PET scan. Uncorrected beam hardening and scatter build-up reduces measured attenuation along the lines of high attenuation between the arms.

CONCLUSION

On the basis of this preliminary study, we conclude that use of 3-mm copper filter to harden the X-ray beam is optimal for removing the artifacts without causing any significant reduction in the photon flux of the resulting X-ray beam. We found that image quality has improved significantly with almost no artifact, which is a very common problem seen in inadequately filtered X-ray beams. Significant improvements in the CNR and spatial resolution were also noticed in all image sets acquired with 3-mm additional copper filter. We propose that as artifacts have been removed from the images, the value of Hounsfield units will be more accurate and hence the value of attenuation coefficients lead to better spatial resolution, contrast and visualization of SPECT images. We wish to extend this work to see the effect of improved attenuation map on the SPECT images.

REFERENCES

1. Radon J. Uber die bestimmung von funktionen durch ihre integralwerte langs gewisser manningfaltikeiten (on the determination of functions from the integrals along certain manifolds). Berichte Saechsische Akademie der Wissenshaft 1917;29:262-77.
2. Cormack AM. Representation of a function by its line integrals with some radiological applications. J App Phys 1963;34:2722-7.
3. Cormack AM. Representation of a function by its line integrals with some radiological applications II. J App Phys 1964;35:2908-13.
4. Kuhl DE, Edwards RQ. Image separation radioisotope scanning. Radiology 1963;80:653-62.
5. Hounsfield GN. Computerized transverse axial scanning (tomography): Part 1. Description of the system. Br J Radiol 1973;46:1016-22.
6. Budinger TF, Gullberg GT. Three-dimensional reconstruction in nuclear medicine emission imaging. IEEE Trans Nucl Sci 1974;21:2-20.
7. Budinger TF, Gullberg GT. Transverse section reconstruction of X-ray emitting radionuclides in patients. Reconstruction tomography in diagnostic radiology and nuclear medicine. Baltimore: University Park Press; 1977. p. 315-42.
8. Budinger TF, Gulberg GT, Huesman RH. Emission computed tomography, In: Herman GT, editor. *Topics In* Applied Physics, Image Reconstruction From Projections, Implementation And Application. New York: Springer Verlag; 1979. p. 147-246.
9. Gustafson DE, Berggren MI, Singh M and Dewanjee MK. Computed transaxial imaging using gamma emitters. Radiology 1978;129:187-94.
10. Larsson SA. Gamma camera emission tomography. Acta Radiol suppl 1980;363:1-75.
11. Beekman FJ, Kamphuis C. Effects of truncation of transmission projections on cardiac SPECT images acquired by a right-angle dual-camera with half-fan-beam collimators. IEEE Trans Nucl Sci 1998a;45:1174-8.
12. Tan P, Bailey DL, Meikle SR, Eberl S, Fulton RR, Hutton BF. A scanning line source for simultaneous emission and transmission measurements in SPECT. J Nucl Med 1993;34:1752-60.
13. Heller EN, Deman P, Liu YH, Dione DP, Zubal IG, Wackers FJ, *et al.* Extra cardiac activity complicates quantitative cardiac SPECT imaging using a simultaneous transmission-emission approach. J Nucl Med 1997;38:1882-90.
14. Almquist H, Arheden H, Arvidsson AH, Pahlm O, Palmer J. Clinical implementation of down-scatter in attenuation-corrected myocardial SPECT. J Nucl Card 1999;6:406-11.
15. Gupta AK, Nelson RC, Johnson GA, Paulson EK, Delong DM, Yoshizumi TT. 2003 Optimization of eight-element multi-detector row helical CT technology for evaluation of the abdomen. Radiology 2003;227:239-45.
16. Nuyts J, Stroobants S, Dupont P, Vleugels S, Flamen P, Mortelmans L. Reducing loss of image quality due to the attenuation artifact in uncorrected PET whole body images. J Nucl Med 2002;43:1054-62.
17. Lang TF, Hasegawa BH, Liew SC, Brown JK, Blankespoor SC, Reilly SM, *et al.* Description of a prototype emission-transmission computed-tomography imaging system. J Nucl Med 1992;33:1881-7.
18. Hamann M, Aldridge M, Dickson J, Endozo R, Lozhkin K, Hutton BF. Evaluation of a low-dose/slow-rotating SPECT-CT system. Phys Med Biol 2008;53:2495-508.
19. LaCroix KJ, Tsui BMW, Hasegawa BH, Brown JK. Investigation of the use of X-ray CT images for attenuation compensation in SPECT. IEEE Trans Nucl Sci 1994;NS-41:2793-9.
20. Blankespoor SC, Xu X, Kalki CK, Brown JK, Tang HR, Cann CE, *et al.* Attenuation correction of SPECT using X-ray CT on an emission-transmission CT system: Myocardial perfusion assessment. IEEE Trans Nucl Sci 1996;NS-43:2263-74.
21. Fricke H, Fricke E, Weise R, Kammeier A, Lindner O, Burchert W. A method to remove artifacts in attenuation-corrected myocardial perfusion SPECT introduced by misalignment between emission scan and CT-derived attenuation maps. J Nucl Med 2004;45:1619-25.
22. Fricke E, Fricke H, Weise R, Kammeier A, Hagedorn R, Lotz N, *et al.* Diethelm tschoepe and wolfgang burchert, attenuation correction of myocardial SPECT perfusion images with low-dose CT: Evaluation of the method by comparison with perfusion PET. J Nucl Med 2005;46:736-44.
23. Kinahan PE, Hasegawa BH, Beyer T. X-ray-based attenuation correction for positron emission tomography/computed tomography scanners. Semin Nucl Med 2003;23:166-79.

How to cite this article: Kheruka SC, Naithani UC, Maurya AK, Painuly NK, Aggarwal LM, Gambhir S. A study to improve the image quality in low-dose computed tomography (SPECT) using filtration. Indian J Nucl Med 2011;26:14-21.

Source of Support: Nil. **Conflict of Interest:** None declared.